CANCER BIOTHERAPY AND RADIOPHARMACEUTICALS
Volume 29, Number 10, 2014

DOI: 10.1089/cbr.2014.1718

Enhanced Singlet Oxygen Production by Photodynamic Therapy and a Novel Method for Its Intracellular Measurement

Sandra L. Pena Luengas,[1] Gustavo Horacio Marin,[2] Kevin Aviles,[3] Ricardo Cruz Acuña,[4] Gustavo Roque,[2] Felipe Rodríguez Nieto,[5] Francisco Sanchez,[6] Adrián Tarditi,[2] Luis Rivera,[1] and Eduardo Mansilla[2]

Abstract

The generation of singlet oxygen (SO) in the presence of specific photosensitizers (PSs) or semiconductor quantum dots (QDs) and its application in photodynamic therapy (PDT) is of great interest to develop cancer therapies with no need of surgery, chemotherapy, and/or radiotherapy. This work was focused on the identification of the main factors leading to the enhancement of SO production using Rose Bengal (RB), and Methylene Blue (MB) as PS species in organic and aqueous mediums. Subsequently, the capacity of zinc oxide (ZnO), zinc sulfide (ZnS), and ZnO/ZnS core-shell QDs as well as manganese (Mn^{+2}) doped ZnO and ZnS nanoparticles (NPs) as potential PS was also investigated. Many variable parameters such as type of quencher, PSs, NPs, as well as its different concentrations, light source, excitation wavelength, reaction time, distance from light source, and nature of solvent were used. The degradation kinetics of the quenchers generated by SO species and the corresponding quantum yields were determined by monitoring the photo-oxidation of the chemical quencher and measuring its disappearance by fluorometry and spectrophotometry in the presence of NPs. Small intracellular changes of SO induced by these metal Zn (zinc) NPs and PDT could execute and accelerate deadly programs in these leukemic cells, providing in this way an innovative modality of treatment. In order to perform further more specific *in vitro* cytotoxic studies on B-chronic lymphocytic leukemia cells exposed to Zn NPs and PDT, we needed first to measure and ascertain those possible intracellular SO variations generated by this type of treatment; for this purpose, we have also developed and tested a novel method first described by us.

Key words: B-CLL, chemotherapy, lymphoma, targeted therapy, treatment

Introduction

Photodynamic therapy (PDT) has been used as a noninvasive procedure for treating a variety of different tumors, including skin, esophageal, bladder, lung, and cervical cancers,[1] and many nontumoral disease conditions such as age-related macular degeneration.[2] Singlet oxygen (SO) is believed to be the major cytotoxic agent involved in PDT.[3] We have reviewed current methods for generating SO[4] and have found that the proper amounts of light, photosensitizer (PS), and/or oxygen influence the SO generation efficiency.[5] The photosensitizing capacity of any compound is dependent on its SO yield (Q_Δ),[6,7] as well as on the so-called triplet-state yield (Φ_t); that is, the probability that a PS, after absorption of a quantum of light, will be converted to the T1 state or first excited triplet state of PS.[8] Triplet-state energy (ΔE_t) reflects the difference between the energies of the S0 and T1 states of the PS.[9,10] A final parameter is the ability to generate SO per

[1]Department of Chemistry, University of Puerto Rico, Puerto Rico.
[2]Tissue Engineering, Regenerative Medicine and Cell Therapies Laboratory, CUCAIBA, La Plata, Argentina.
Departments of [3]Biology and [4]Chemical Engineering, University of Puerto Rico, Puerto Rico.
[5]Department of Chemistry, Jauretche University, Florencio Varela, Argentina.
[6]School of Physics, National University of La Plata, La Plata, Argentina.

Address correspondence to: Sandra L. Pena Luengas; Department of Chemistry, University of Puerto Rico; Mayagüez Campus, Puerto Rico
E-mail: **sandraluengas@yahoo.es**

irradiation power and PS concentration ($\alpha = 1.925 \times 10^{-5}\ \lambda\ \Phi_\Delta\ \varepsilon$), where λ is irradiation wavelength and ε is the molar extinction coefficient of the PS at the wavelength used, expressed in $M^{-1}\ cm^{-1}$, where Φ_Δ is the SO quantum yield (QY).[6,11] This quantity is defined as the number of SO molecules generated for each photon absorbed by the PS. Each PS molecule can produce 10^3–10^5 molecules of SO before being degraded.[5] Φ_Δ have been determined relative to the known value for a reference substance. Undesirable deleterious effects such as the photo-bleaching of the PSs and/or the quenchers, as well as the physical quenching of the excited states could be predicted from nonevaluating light parameters (wavelength of excitation, light intensity, and photon density); it could not be completely possible to explain the negative effects of the absence of appropriate quantities of PS, light, or oxygen on SO generation. To this end, it was needed to have a PS/quencher system that would uniquely produce SO by the Type II mechanism for PDT applications.[12] It has been shown that SO is the responsible species for the selective destruction of malignant tumor cells, and it has been recognized that the therapeutic efficiency of PDT may be completely reversed depending on whether Type I or Type II mechanisms are operating.[13] Thus, it is imperative to have a PS/quencher pair system in which its main photo-oxygenation pathway would be of the Type II mechanism, which is well known to produce SO only.[14] On the other hand, a Type I mechanism is that in which the excited state sensitizer activates the substrate directly, usually by electron or hydrogen abstraction.[14] Only in a Type II mechanism, the excited-state sensitizers can generate excited singlet-state oxygen by energy transfer.[15] Then, SO can oxidize the ground-state substrate. Many dyes possess triplet state of appropriate energies and can sensitize production of SO.[16] Two of these dyes that are most commonly used for photochemical generation of SO are Rose Bengal (RB) and Methylene Blue (MB).[17,18] The nature of the reaction mechanism depends on the oxidation potential of the chosen PS as well as on the quencher[8]; then, the formation of products derived from either Type I or Type II will be determined accordingly. We have focused our attention on enhancing the SO production from quenchers known to be sufficiently reactive and whose reaction products have been elucidated in the literature.[20] In this way, we choose to study the photo-oxygenation of 1,3-diphenylisobenzofuran (DPBF) and 2,5-diphenylfuran (DPF)[19] using two well-known photosensitizers, RB and MB. Both DPF and DPBF have been found to self photo-oxidate through absorption in the ultra violet (UV) region so that visible excitation light has to be used in both cases to avoid the auto-oxidation processes.[20] No systematic comparative studies on the effect of light sources with distinct characteristics for irradiation wavelengths and power have been reported, especially for *in vitro* versus *in vivo* experiments. Isolated reports on the use of light-emitting diode (LED) and LED lasers have appeared in the scientific literature,[3,21] but no systematic studies have been reported about the correlation of LED and LED laser intensities with levels of SO production for standard organic dyes used as sensitizers. B-chronic lymphocytic leukemia (B-CLL) is the most common adult leukemia in the western world and usually follows an adverse, relentless clinical course by slowly developing drug resistance to fludarabine and other chemotherapeutic agents, as well as by acquiring new different genetic abnormalities.[22] At this stage, B-CLL will not have any possible curative therapeutic option.[23] Considering that B-CLL cells as many other cancer cells may have an altered redox state spontaneously producing higher amounts of ROS in relation to normal ones,[24,25] a strategy using Zn nanoparticles (NPs) and PDT could be a specific and novel optional effective treatment even for resistant phenotypes of this disease, specially if increased levels of intracellular SO induced by its action could be detected. Measurement of SO in biological environments has been a major task, especially when intracellular values, without interferences from the external medium, were required. Near-infrared (NIR) luminescence at 1270 nm in cell environments is confounded by the strongly reduced SO lifetime and probably had never been achieved until a research group developed an NIR-sensitive photomultiplier tube probe that allowed to clearly identify and measure a true intracellular component of SO signal.[26] However, all these few described methods are expensive and required a complex technology to be performed.[27,28] The possibility to develop a simple, inexpensive technique for the measurement of intracellular variations of SO production could be a must in the evaluation of novel anticancer therapies, especially those using metal NPs and PDT. Our main objectives were to evaluate the solvent nature, light source for energy requirements, intensity of light source, and the effects of oxygen quenching with regard to improving SO generation. In addition, there are benefits of using a broad versus a specific wavelength excitation source as well as an LED or a laser LED as excitation sources. All of this is done with the ultimate goal of developing precise, sensitive, and reproducible methods to enhance the generation of SO from inorganic NPs in organic and aqueous mediums, but, more importantly, to finally test all this acquired knowledge in a B-CLL cell *in vitro* cell model[29] by designing an effective simplified measurement method to detect minimal changes in intracellular SO levels.

Materials and Methods

Photo-oxidation reactions

Experimental set-up for photo-oxidations consisted of a light source, a quartz cuvette, a dark black box, a spectrophotometer (UV-visible DU 800 Shimadzu), and a spectrofluorometer (FluoroMax2) with a 150 mW continuous ozone-free Xe lamp as the excitation source. The samples were analyzed by UV-visible (UV-vis) spectroscopy and fluorometry immediately after irradiation with the specified light source. MB and RB 97%, DPBF 97%, DPF 97%, L-histidine 97%, imidazole 97%, and DPBF 97% were used without further purification; methanol (ultrapure high-performance liquid chromatography [HPLC] grade, 99.8 + %) and nanopure water were also used (all purchased from Sigma-Aldrich).

Determination of SO

1. Individual stock solutions of PS at 1×10^{-5} M, NPs at 15 μg/mL, and quencher at 6.0×10^{-5} M for DPBF and (DPF) were prepared. Using *p*-nitrosodimethylaniline (RNO) as a selective, scavengers were prepared at 50 μM plus Histidine at 0.01 M or imidazole at 8 mM.

2. Two milliliters of PS or NP and 1 mL of quencher were mixed without exposing to light and placed inside a quartz cuvette in a dark black box that was especially constructed for these purposes before exciting the mixture with a light source and analyzed by UV-vis spectroscopy and fluorescence at ''zero time'' before irradiation.
3. Controls with only the quencher, photosensitizer, and NPs were made.
4. Absorbance and fluorescence data were collected every 2 seconds for a total time of 10 seconds of laser irradiation with a rest period between irradiations of 2 minutes. Experiments were made in triplicate. Different irradiation times were evaluated for *in situ* generation of SO, and the samples were saturated with air.
5. Similarly, we measured the intracellular production of SO as described earlier in B-CLL cells. Four million leukemic cells/2 mL of phosphate-buffered saline (PBS) were incubated with the selected concentration of NPs and DPBF at 6.0×10^{-5} M, during the selected incubation time and later analyzed by fluorescence.

Since DPBF is very sensitive to photobleaching, it was always diluted in dark flasks and mixed with the PSs or NPs only immediately before taking the samples at ''0 time.'' Samples were collected at specified time intervals, and UV-vis as well as fluorescence spectra were recorded for each sample taken at those time points. Analysis of the experimental results was performed by modifying a procedure reported by Dumas et al.[11] using plots of 1/ratio (A) versus 1/A, where A corresponds to the absorption of DPBF at 410 nm and ratio (A); the variation of absorbance of the solution at a wavelength specific to DPBF ($\lambda = 410$ nm) after the irradiation step for each of the individual sets of reactions runs with different light sources. The ratio (A) values used were the quotients of the absorbance values for DPBF divided by the respective absorbance values for the specific PS. From the resulting straight lines obtained for 1/ratio (A) = f(1/A), we characterized the formation of SO and determined the parameter β. The β values can be considered an index of reactivity of particular organic compounds with SO.[30] A lower value means that a higher concentration of acceptor is needed for oxygenation or that the reaction is slower under the reaction conditions.

Synthesis of NPs

Eight different types of Zn NPs were synthesized by different methods as described here: NP1 ZnO, NP2 ZnO:Mn 0.5%, NP3 ZnO:Mn 1.0%, NP4 ZnO:Mn 1.5%, NP5 ZnO:Mn 2.0%, NP6 ZnS, NP7 ZnS:Mn 1.0%, and NP8 ZnO/ZnS. NPs were finally diluted and prepared for all experiments by vigorous sonication and addition of human albumin (1.5 mg/mL) to disaggregate them.[31,32]

Synthesis of ZnO and Mn-doped ZnO NPs

These NPs were synthesized via wet-chemical techniques.[33,34] Briefly, 4 mmol of Zn acetate were dissolved in 40 mL of ethanol and heated at 50°C with intense stirring for 30 minutes, with this one being the precursor ''A.'' Then, 4 mmol of sodium hydroxide (NaOH) were dissolved in 40 mL of ethanol and heated at 50°C along with vigorous stirring for 1 hour, making in this way precursor ''B.'' Next, 0.02 mmol of manganese acetate (dopant) were dissolved in 40 mL of ethanol at 50°C along with vigorous stirring for 30 minutes to produce precursor ''C.'' Then, 20 mL of precursor ''A'' were mixed with 20 mL of precursor ''C.'' Both solutions were heated at 80°C for 30 minutes. After cooling, 20 mL of precursor ''B'' were finally added to the mixed solution with constant stirring. The new solution was kept in an oil bath at 65°C for 2 hours. After cooling for 4 hours, the solution was centrifuged for 20 minutes at 4000 rpm. The precipitate was washed and dried. The different Mn doping percentages applied on the surface of NPs were 0.5%, 1.0%, 1.5%, and 2.0%. Un-doped ZnO NPs were synthesized with a similar procedure except for the addition of Mn acetate (Zinc acetate dihydrate, sodium sulfide nonhydrate, manganese acetate tetrahydrate, and sodium hydroxide were purchased from Sigma-Aldrich.).

Synthesis of colloidal ZnS semiconductor nano-crystals was capped with poly-vinyl-pyrrolidone (PVP) and prepared using a 1% concentration of Mn^{+2} ion as a dopant:

The NPs were synthesized via wet-chemical techniques.[35,36] Aqueous solutions of 1.0 M $Zn(C_2H_3O_2)_2$, 0.85 M Na_2S, and 0.010 M $Mn(C_2H_3O_2)_2$ were prepared. Next, 0.56 g of (PVP) was dissolved in 5 mL of the zinc acetate solution obtaining a concentration of 1.0 M. Five milliliters of the manganese acetate solution was then added to this mixture. Five milliliters of the sodium sulfide solution was finally mixed slowly with continous stirring, thereby precipitating the NPs. The solution was centrifuged for 10 minutes at 3000 rpm and washed with deionized water. The nano-crystals were re-dispersed in water to make a 0.01 M solution. Un-doped ZnS NPs were synthesized with a similar procedure except for the addition of manganese acetate.[35] [Zinc acetate dihydrate, sodium sulfide nonahydrate, manganese (II) acetate tetrahydrate, and PVP were purchased from Sigma-Aldrich.]

Preparation of ZnO/ZnS core shell NPs

The preparation of ZnO/ZnS core shell NPs was performed by thermal decomposition of Zn-MPA (3-mercaptopropionic acid) complexes.[37,38] Briefly, 10 mL of a 0.1 M $Zn(C_2H_3O_2)_2\cdot 2H_2O$ aqueous solution and 0.35 mL of MPA were mixed in a flask. This solution was diluted to 98 mL with water; the pH was adjusted to 10.3 with 4 M NaOH and saturated with nitrogen (N_2) by bubbling for 20 minutes. ZnO NPs were dispersed in water to obtain a concentration of 0.01 M, diluted to 43 mL again with water, and purged with N_2. Seven milliliters solution of Zn^{+2}-MPA complex was added dropwise to ZnO quantum dots (QDs), and the mixture was refluxed for 6 hours. NPs were recovered by filtration and dried in an oven at 60°C (Zinc acetate dihydrate, 3-mercaptopropionic acid, and sodium hydroxide were purchased from Sigma-Aldrich.).

Chromatographic separations

Chromatographic conditions were carried out using an Agilent 1100 Series HPLC, a diode array detector (DAD), and a temperature control module. Separations were performed with a C18 analytical column maintained at 25°C. RB, DPBF, and the final product were obtained by photooxidation: *o*-dibenzoylbenzene was separated by means of reversed-phase liquid chromatography, using a gradient

mobile phase of 90% acetonitrile and 10% water at a flow of 1.0 mL/min. A direct injection was used for detection in which 20 μL of sample were injected. The samples were filtered before injection to remove any particulate matter. The concentrated analytes were desorbed into an HPLC column followed by separation.

Procurement and manipulation of cells

B-CLL cells were obtained after informed consent from 1 patient and isolated from blood by density gradient centrifugation, using a Ficoll–Hypaque separation technique followed by a highly specific purifying method using a B-Cell Isolation Kit developed for the fast and efficient separation of untouched B cells from human peripheral blood mononuclear cells by negative selection. This is an indirect magnetic labeling system. Non-B cells, for example, T cells, NK cells, dendritic cells, monocytes, granulocytes, and erythroid cells, are indirectly magnetically labeled by using a cocktail of biotin-conjugated antibodies against CD2, CD14, CD16, CD36, CD43, CD235a (Glycophorin A), and anti-biotin micro-beads. Isolation of highly pure B cells is achieved by depletion of magnetically labeled cells using MACS® columns from Miltenyi Biotec GmbH.[39] For all experiments 2×10^6 cells per mL were incubated at 37°C/5% CO_2 in RPMI 1640 medium with 10% fetal bovine serum (Invitrogen) and immediately used after centrifugation and resuspension in PBS.

Tested NPs in cell experiments

From the eight NPs produced, we cell tested *in vitro* only two NPs, one from the ZnO group: ZnO:Mn^{+2} 1.0% doping (NP3) and one from the ZnS group:ZnS (NP6). All the experiments were performed with 15 μg/mL of NPs in PBS.

PDT procedures on B-CLL cells cultured with NPs

PDT was implemented by the use of a green laser (EVO Series-3B-Wicked Laser) with a wavelength of 532 nm and 75 mW of power in order to irradiate the samples. The sample containing 4 million cells in 2 mL of PBS was incubated with NPs and DPBF as the chemical quencher.[20] The concentration of DPBF used in these probes was 6.0×10^{-5} M and for NPs, it was 15 μg/mL. After the selected time of 2 hours for cell incubation with NPs and the quencher at complete darkness, the samples with a total volume of 2 mL were mixed in a quartz cuvette and immediately irradiated with the laser light source. The light laser was kept constant at 40 cm from the samples in order to irradiate them inside a dark black box that was especially constructed for these purposes. We used a standard photosensitizer of a known SO QY, RB, at 1.0×10^{-5} M with a high QY of SO ($\Phi_\Delta=0.75$).[40,41] Then, SO QYs were determined by monitoring the disappearance of the quencher's bands from their respective photoluminescence spectra, using an excitation of 410 nm under continuous irradiation and by using a novel method first described by us. Fluorescence was measured with a spectrofluorometer (FluoroMax2) with a 150 mW continuous ozone-free Xe lamp as the excitation source. Fluorescence data were collected every 2 seconds and for a total approximate time of 14 seconds of laser irradiation with a rest period between irradiations of 2 minutes.

Measurement of intracellular SO production

For the measurement of intracellular SO production and its variations, a novel and innovative method was thought of and implemented by us. Briefly, determination of the intracellular SO generation QY after incubation of B-CLL cells with NPs was done by fluorometry quantitative analysis of photo-oxidation reactions using DPBF at 6.0×10^{-5} M as the quencher, after the administration of PDT. Incubation of cells with DPBF was done for 2 hours. Then, centrifugation of the cells was done in complete darkness for 40 minutes, followed by determination of the presence of any residual DPBF in the supernatants by fluoroscopic measurement. After this, re-suspension of the cells in new PBS was done with centrifugation for another 30 minutes two more times, exchanging every time the supernatant by new PBS. Measurement of no residual DPBF was supposed to be reached in the final supernatant, or more cycles of washing and centrifugation were performed until no trace of DPBF could finally be found in it. At the end, re-suspension of cells in new PBS and measurement of intracellular emission at DPBF wavelength by fluoroscopy analysis was performed after PDT. By using DPBF, at a nontoxic concentration for B-CLL cells, we observed and registered the changes in its levels, especially the decrease of its fluorescence emission intensity, in a time-dependent manner. The method used to calculate the production of intracellular SO when DPBF performed as the chemical quencher in a decomposition reaction was done by the analysis of DPBF oxidation by SO using the Equation (1)[42]: $\Phi\Delta sample = \Phi\Delta refKsample/Kreference$, in which $\Phi\Delta ref$ is SO QY of RB, Ksample and Kreference are the slopes of the plot of the time-dependent decomposition of DPBF, expressed as the decrease of fluorescence at 457 nm of the measured NPs and the RB, respectively. In this way, SO production was detected in B-CLL cells when treated with NPs and PDT.[43,44]

Statistical analysis

Data were expressed as mean plus or minus the 95% confidence interval. *T*-test was used to compare the mean values of the different experimental groups and control samples. The one-way analysis of variance (ANOVA) was used to compare the values of the control samples with sample time points of B-CLL cells at 24 hours of incubation with NPs and PDT treatment. *p*-Values <0.05 were considered statistically significant.

Results and Discussion

Photo-oxygenation of DPBF and DPF with RB and MB, respectively

Several sensitizer/quencher combinations were studied, and the experimental parameters and reaction conditions were evaluated (wavelength of absorption monitored, light source, intensity of light source, and irradiation time), as well as the reaction conditions for the photo-oxygenation for the DPBF and DPF quenchers. Time-dependent decomposition of DPBF in methanol photosensitized by RB and MB irradiated with a 5 W LED flashlight and 5 mW laser LED, respectively, 5 cm from light source every 10 seconds for a total of 50 seconds for comparison, showed an excellent

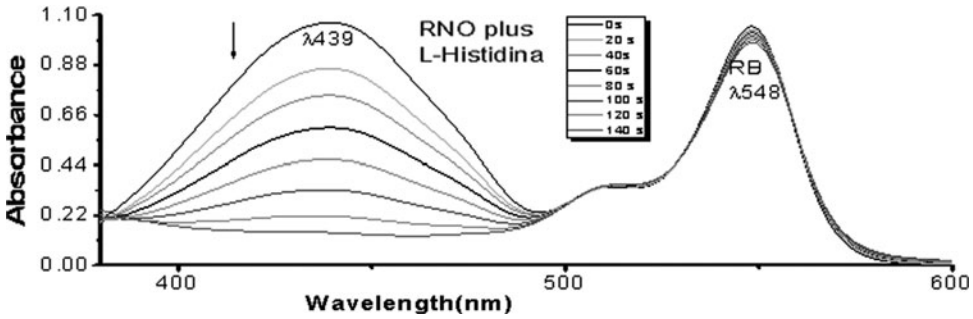

FIG. 1. Absorption spectra photo-oxidation of RNO at 50 μM plus L-histidine at 0.01 M in presence of Rose Bengal (RB) at 1×10^{-5} M in water. The sample was irradiated with a 200 mW laser at a distance of 5 cm every 20 seconds for approximately 140 seconds while stirring at 340 rpm with the addition of 10 mL air.

linear correlation, indicating higher SO production for RB compared with MB ($p<0.05$). The photo-oxidation results using a white light source (incandescent and fluorescent white light bulbs) compared favorably with those using white light LEDs and specific wavelength LED lasers. It was also clearly observed by spectrophotometric analysis that the photo-oxidation of DPBF when sensitized by MB in methanol and irradiated every 10 seconds for a total of 140 seconds produced a diminished absorption with time, as it was consumed by SO. On the other hand, UV-vis spectra for the photo-oxidation of DPBF with MB in methanol with the addition of air using a 67 mW red LED laser in which irradiation was delivered for just 1 minute eliminated almost completely the DPBF signal at 410 nm, evidencing a much faster reaction with a higher intensity light source. Note that pure oxygen or air is also well known to enhance the rate of Type II photoxidation.[45,46] RB showed both a higher β and reaction constants[47] than MB using DPBF as a quencher ($p<0.05$). In addition, a comparison of the respective slopes of the DPBF decomposition curves with the corresponding light intensities used showed that definitely the LED lasers outputs correlated well with the increased photo-oxidation rates and, thus, significantly enhanced the SO production with a higher better performance than that observed with the white light fluorescent bulb.

The time-dependent decomposition of DPF was also studied by irradiating with a 5 mW LED laser sensitized by RB and MB, a 13 W fluorescent light bulb sensitized by RB and MB at different time intervals, and 5 and 67 mW LED lasers sensitized by MB. In all cases, an excellent linear correlation was observed between a decrease in DPF absorption band with time and RB, exhibiting a higher reaction rate than that observed using MB ($p<0.05$). For the photo-oxidations involving LED lasers with different intensities, a much more faster reaction was observed with the higher intensity LED laser in every case ($p<0.05$) In addition, the reaction occurred faster at closer distances from the light source (2.5 vs. 5 cm) for the 67 mW LED laser.

The bleaching of RNO in the presence of histidine or imidazole

In addition, we used another indirect method based on the quenching of a substrate (imidazole or histidine) with SO after irradiation of the nitroso RNO compound at 440 nm. The photosensitizers used were (RB) and (MB), and the following experimental parameters were evaluated: wavelength of absorption monitored, light source, intensity from light source, and irradiation time for RNO quencher. All photo-oxidations reactions were done after addition of 10 mL of air with a gas syringe into the sample. The UV-vis spectra of RNO at 50 μM plus L-histidine at 0.01 M in the presence of RB and MB, respectively, at 1×10^{-5} M. using aerated aqueous solutions, and irradiated with a 200 mW-green laser 532 nm for RB and a red laser 650 nm for MB were performed (Figs. 1 and 2). UV-vis data were collected every 20 seconds for 140 seconds for RB and 100 seconds for MB. The bleaching of RNO was induced by the reaction of SO with L-histidine. A trans-annular peroxide was produced between the reaction of SO with L-histidine and caused the bleach of RNO at 439 nm.[48] We have also tested the system RNO plus imidazole at 8 mm, obtaining the bleaching of RNO induced by the reaction between SO and imidazole.

When the time-dependent decomposition of RNO plus L-histidine was evaluated by SO in water using RB and MB, and of RNO plus imidazole by SO in water using RB and MB, there was an excellent linear correlation in all cases, with time being indicative of a first-order kinetic reaction with regard to a decrease in imidazole and L-histidine concentrations with time. In addition, in both cases when

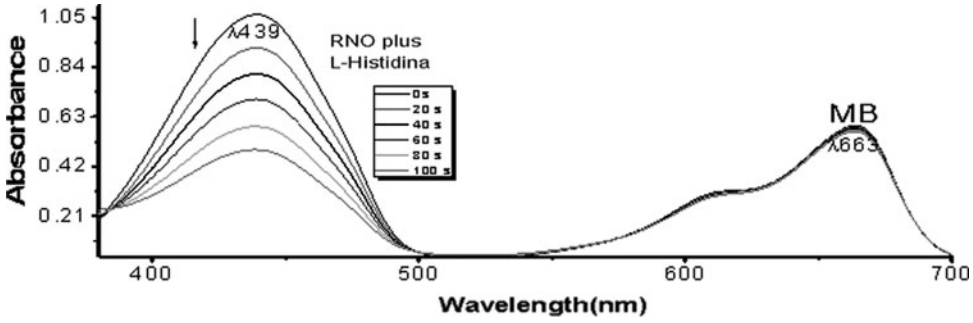

FIG. 2. Absorption spectra photo-oxidation of RNO at 50 μM plus L-histidine at 0.01 M in presence of Methylene Blue (MB) at 1×10^{-5} M in water. The sample was irradiated with a 200 mW laser at a distance of 5 cm every 20 seconds for approximately 100 seconds while stirring at 340 rpm with the addition of 10 mL air.

RNO plus L-histidine or RNO plus imidazole was tested, a higher SO production was always observed with RB over MB ($p < 0.05$). The SO QY results were obtained for RB and MB in water using RNO/imidazole and RNO/L-histidine quenchers and light sources at 5 cm from the samples. The SO QYs were determined for RB and MB using Equation (1): $\Phi\Delta sample = \Phi\Delta ref \times Ksample/Kref$, which uses the slope from the time-dependent decomposition of RNO plus L-histidine by SO in water for one sensitizer, RB or MB, and the SO QY value from the literature of one sensitizer to calculate the SO QY of the other from its slope obtained from the time-dependent decomposition of RNO plus L-histidine by SO in water. In an analogous manner, the SO QY of a sensitizer can be calculated, RB or MB for the decomposition of RNO plus imidazole by SO in water. The SO QYs obtained in this case were lower for MB than for RB, similar to the results obtained for the photo-oxidation of DPBF and DPF quenchers in methanol. SO production was higher using RB compared with MB ($p < 0.05$). L-Histidine and imidazole reacted with SO, causing a progressive decrease in the intensity of RNO. The RNO bleaching by the use of RB or MB was a time-dependent phenomenon. Then, it was clear that a similar phenomenon was observed in both cases when DPBF or DPF were used as chemical scavengers in methanol, respectively.

HPLC analyses

HPLC was utilized to evaluate the identity of the reaction photoproducts and photo-oxidation rates with RB and DPBF as a quencher. The sample was irradiated with a 5 mW-green laser 532 nm at a distance of 5 cm every 20 seconds for approximately 60 seconds. All the analytes were separated efficiently by reverse-phase chromatography with a DAD, which included the *o*-dibenzoylbenzene, DPBF, and the unreacted RB sensitizer. A linear correlation was obtained by plotting the DPBF quencher area ratio A_t/A_0 versus time in seconds, which indicated a first-order reaction.

After optimizing the conditions for PSs to produce SO, we moved to experiments with NPs in order to quantify the production of SO for all the NPs mentioned earlier, using two methods: spectrophotometry and fluorometry. All experiments were made in triplicate. The ZnO NPs analyzed were 0.5%, 1.0%, 1.5%, and 2.0% Mn doped ZnO NPs and the core-shell ZnO/ZnS NPs, as well as the ZnS and the 1.0% Mn doped ZnS NPs. Similar results were obtained by both methods for NPs of 1.0% and 1.5% Mn doped ZnO and 1.0% Mn doped ZnS NPs. Core-shell ZnO/ZnS did not produce SO at all (Table 1). The experimental conditions for measuring production of SO by both methods were as follows: 15 μg/mL in water of NPs, the concentration of DPBF was 6.0×10^{-5} M, and the sample was irradiated with a green laser of 532 nm and 75 mW of power every 2 seconds for approximately 10 seconds and a stir of 340 rpm. It was necessary to add 10 mL of air with a gas syringe to every sample to ensure the presence of oxygen in the medium.

Table 1. Singlet Oxygen Quantum Yield of Nanoparticles by Spectrophotometric and Fluorometric Analysis of DPBF Oxidation in Water

NPs	Φ_Δ *SO by spectrophotometry analysis*	Φ_Δ *SO by fluorometry analysis*
ZnO	N.R.	0.71 $p < 0.05$
ZnO:Mn^{+2} 0.5% doping	0.60 $p < 0.05$	0.48
ZnO:Mn^{+2} 1.0% doping	0.32	0.28
ZnO:Mn^{+2} 1.5% doping	0.17	0.17
ZnO:Mn^{+2} 2.0% doping	N.R.	0.1
ZnS	0.36	0.22
ZnS:Mn^{+2} 1.0% doping	0.20	0.23

NPs, nanoparticles; N.R., values detected at very low levels or nonrecorded; SO, singlet oxygen.

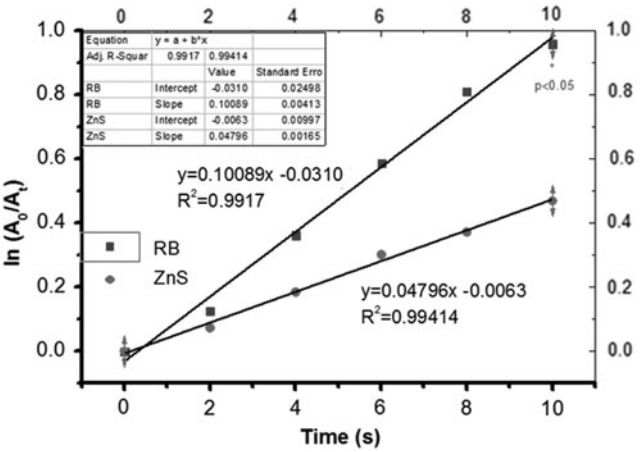

FIG. 3. Time-dependent decomposition of DPBF at 6.0×10^{-5} M by singlet oxygen (SO) produced by ZnS nanoparticles (NPs) at 15 μg/mL in water and irradiated with a 75 mW laser at a distance of 40 cm for approximately 10 seconds every 2 seconds compared with that produced by RB under same experimental conditions (spectrophotometric method).

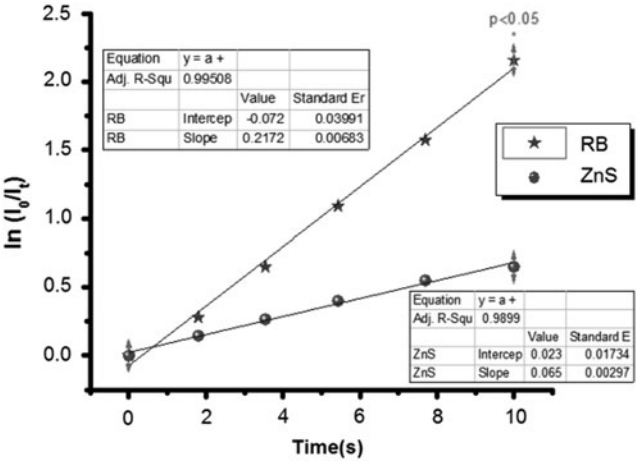

FIG. 4. Time-dependent decomposition of DPBF at 6.0×10^{-5} M by SO produced by ZnS NPs at 15 μg/mL in water and irradiated with a 75 mW laser at a distance of 40 cm for approximately 10 seconds every 2 seconds compared with that produced by RB under same experimental conditions (fluorometric method).

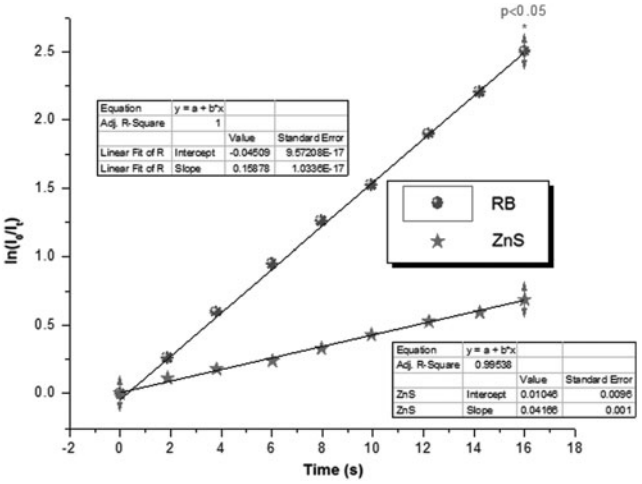

FIG. 5. Time-dependent decomposition of DPBF at 6.0×10^{-5} M by SO produced by ZnS NPs at 15 μg/mL and RB at 1.0×10^{-5} M, incubated with B-chronic lymphocytic leukemia (B-CLL) cells (4 million/2 mL phosphate-buffered saline [PBS]), and irradiated with a laser 532 nm at a distance of 40 cm for approximately 16 seconds every 2 seconds compared with that produced by RB under same experimental conditions (fluorometric method).

Absorption and fluorescence spectra photo-oxidation of DPBF in the presence of 1.0% Mn doped ZnO and ZnS NPs at 15 μg/mL in water showed that DPBF reacted with SO, causing a progressive decrease in the intensity of the quencher. This decomposition of DPBF by SO produced by the use of 1.0% Mn doped ZnO and ZnS NPs at 15 μg/mL with laser irradiation was a time-dependent phenomenon by both methods: spectrophotometric (Fig. 3) and fluorometric (Fig. 4). The QY was calculated using Equation (1).[42] This method, as it was said earlier, used a standard PS of a known

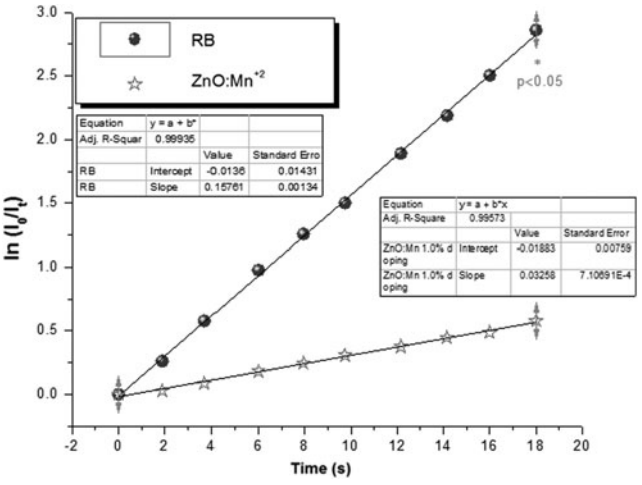

FIG. 6. Time-dependent decomposition of DPBF at 6.0×10^{-5} M by SO produced by 1.0% Mn doped ZnO NPs at 15 μg/mL and RB at 1.0×10^{-5} M, incubated with B-CLL cells (4 million/2 mL PBS), and irradiated with a laser 532 nm at a distance of 40 cm for approximately 18 seconds every 2 seconds compared with that produced by RB under same experimental conditions (fluorometric method).

TABLE 2. SINGLET OXYGEN, QUANTUM YIELD OF NANOPARTICLES IN B-CLL LYMPHOCYTIC CELLS

SO QY	*B-CLL lymphocytic cells*
ZnO:Mn^{+2} 1.0% doping (15 μg/mL)	0.16
ZnS (15 μg/mL)	0.21

B-CLL, B-chronic lymphocytic leukemia; QY, quantum yield.

SO QY. In our case, we used RB at 1.0×10^{-5} M with a high QY of SO ($\Phi_\Delta=0.75$).[47] SO QY of RB was significantly higher compared with QY of NPs (Fig. 4; $p<0.05$).

Results for all NPs by both methods are presented in Table 1. The highest values of SO QY was 0.60 by the spectrophotometric method using 0.5% Mn doped ZnO NPs ($p<0.05$) and 0.71 by the fluorescence method using ZnO NPs ($p<0.05$). The best results obtained with Mn doped ZnO NPs were those of 0.5% Mn doped concentration measured by both methods. The QY of SO by spectrophotometry was 0.60 and 0.48 by fluorometry, respectively. With increasing doping of ZnO NPs from 1.0% to 2.0%, production of SO decreased. ZnS NPs without Mn doping when compared with 1.0% Mn doped ZnS NPs showed an increased SO production by the spectrophotometric method. The results were similar for ZnS and 1.0% Mn doped ZnS by the fluorometric method. In general, all NPs have a good production of SO and can be used as efficient PS in PDT except ZnO/ZnS core shell.

Intracellular measurement of SO variations after NPs and PDT in vitro *treatment of B-CLL cells*

Fluorescence spectra photo-oxidation of DPBF in the presence of NPs inside B-CLL cells and DPT treatment showed that DPBF reacts with SO, causing a progressive decrease in the intensity of the quencher again. This decomposition of DPBF by SO produced by the use of 1.0% Mn doped ZnO NPs3 and ZnS NPs6 in B-CLL cells was a time-dependent phenomenon (Figs. 5 and 6) with an increased production of intracellular SO in B-CLL cells when PDT was delivered. Intracellular SO QY of RB was significantly higher compared with QY of NPs ($p<0.05$). The QY of SO for B-CLL cells was 0.16 for NPs3 and 0.21 for NPs6 using DPBF as the chemical quencher (Table 2).

Conclusions

PDT has emerged as an important therapeutic option in the management of cancer as well as other diseases.[49] In order to obtain its desired selective killing effect on malignant cells, light-sensitive substances or PS placed in the targeted diseased tissues or cells should be activated by photo-excitation and cytotoxic species such as SO should be produced. In this study, light parameters were evaluated (e.g., intensity of light, broad vs. specific wavelength, and coherent vs. noncoherent nature of light source) for the PSs and quenchers were selected to enhance their effect on SO production. Clearly, as it has been shown here, the best results were obtained with specific wavelength LED lasers that allowed the exact selection of wavelengths and the precise application of light in contrast to lamps, LED flashlights, or fluorescent light bulbs, with this fact being

especially important considering that PDT depends largely on the type of light source used. Important data between fundamental physical properties of light sources and enhanced SO production using standard sensitizers and inorganic NPs have been found and analyzed in order to characterize for the reliable, precise, and reproducible measurement and employment of SO in cancer treatment, especially B-CLL. Our results clearly suggest the strong influence of the LED lasers and light power intensities on the QY of SO in the presence of different PS-quencher photo-oxidation pairs under simultaneous aeration in methanol and water. Besides, RB has been identified both in the literature and in our article as an outstanding PS even better than NPs, especially when only SO production is considered, there are still several technical difficulties in its application with PDT to a wide range of diseases, especially those involving deep tissues, including the blood. Currently, FDA-approved PDT PS absorbed in the visible spectral regions below 700 nm, thus clinically limiting PDT to treating surface and relatively superficial lesions only. It is also usually very difficult to prepare those pharmaceutical formulations that enable parenteral administration of PS, because most of them are hydrophobic, aggregate easily under physiological conditions, and, possibly, have intrinsic toxicities due to their high polarity.[50,51] In this way, NPs such as the ones presented here could offer interesting solutions to each of these difficulties found with the use of traditional PS, including RB. ZnO NPs could participate in the actual mechanism of PDT, mainly by acting as PSs themselves. NPs seem to offer the best hope for extending the reach of this promising therapy to internal organs and tissues in the body, including the hematopoietic system. It is clear now that NPs could provide many advantages over those of traditional PS such as RB. NPs can be active participants in the PS excitation pathways, and also some of them could be considered real PS NPs.[52,53] NPs can be enabled to participate in the radiation mechanisms of PDT for cancer treatment.[51,54] We have also shown that very small variations of intracellular SO concentrations are easily induced by the action of our NPs and PDT in leukemic cells and could be measured by a novel method first described by us. Our intracellular SO measurement method proved to be good enough, reproducible, inexpensive, and quite simple to perform so that it could easily be introduced soon as a routine diagnostic tool. PDT is a clinically tested promising technique to treat cancer and can be associated therapeutically with NPs.[54] In this way, we have now the possibility to use all this knowledge in a larger and more detailed study to fully understand the action of Zn NPs and PDT on B-CLL cells, especially if this strategy could be specifically active in destroying drug-resistant phenotypes of B-CLL cells both *in vitro* and *in vivo* in animal models. If this comes to be true, we could be in front of a new promising treatment not only for human B-CLL and other lymphomas but maybe also to all types of cancer.

Acknowledgments

This work was supported by The National Science Foundation under Grant No. HRD 0833112 University of Puerto Rico, Mayagüez Campus, Nanotechnology Center for Biomedical, Environmental, and Sustainability Applications (UPRM CREST Program).

Disclosure Statement

No financial conflict of interest exists.

References

1. Neubert T, Lehmann P. Bowen's disease: A review of newer treatment options. Ther Clin Risk Manag 2008;4: 1085.
2. Master AM, Livingston M, Oleinick NL, et al. Optimization of a nanomedicine-based silicon phthalocyanine 4 photodynamic therapy (Pc 4-PDT) strategy for targeted treatment of EGFR-overexpressing cancers. Mol Pharm 2012;9:2331.
3. Ricci-Júnior E, Marchetti JM. Zinc(II) phthalocyanine loaded PLGA nanoparticles for photodynamic therapy use. Int J Pharm 2006;310:187.
4. Nakamura K, Ishiyama K, Ikai H, et al. Reevaluation of analytical methods for photogenerated singlet oxygen. J Clin Biochem Nutr 2011;49:87.
5. Jones L, Grossweiner J, Rogers G. The Science of Phototherapy: An Introduction. Springer, 2005, p. 374. Available at: Retrieved from http://books.google.com/books?id=sGZX-Vx6qLQC&pgis=1 Accessed: June 30, 2014.
6. Spiller W, Kliesch H, Wohrle D, et al. Singlet oxygen quantum yields of different photosensitizers in polar solvents and micellar solutions. J Porphyr Phthalocyanines 1998;2:145.
7. De Melo LSA, Gomes ASL, Saska S, et al. Singlet oxygen generation enhanced by silver-pectin nanoparticles. J Fluoresc 2012;22:1633.
8. Schweitzer C, Mehrdad Z, Noll A, et al. Mechanism of photosensitized generation of singlet oxygen during oxygen quenching of triplet states and the general dependence of the rate constants and efficiencies of O 2 (1 Σ g+), O 2 (1 Δ g), and O 2 (3 Σ g -) formation on sensitizer triplet St. J Phys Chem A 2003;107:2192.
9. Zhao J, Wu W, Sun J, et al. Triplet photosensitizers: From molecular design to applications. Chem Soc Rev 2013;42:5323.
10. Washington I, Brooks C, Turro NJ, et al. Porphyrins as photosensitizers to enhance night vision. J Am Chem Soc 2004;126:9892.
11. Dumas S, Leprêtre J-C, Lepellec A, et al. Reactivity of the photo excited forms of Hypericin, Hypocrellin A, Hypocrellin B and methylated Hypericin towards molecular oxygen. J Photochem Photobiol A Chem 2004;163:297.
12. Miller JB. Photodynamic therapy: The sensitization of cancer cells to light. J Chem Educ 1999;76:592.
13. Huang L, Xuan Y, Koide Y, et al. Type I and Type II mechanisms of antimicrobial photodynamic therapy: An *in vitro* study on gram-negative and gram-positive bacteria. Lasers Surg Med 2012;44:490.
14. Ding H, Yu H, Dong Y, et al. Photoactivation switch from type II to type I reactions by electron-rich micelles for improved photodynamic therapy of cancer cells under hypoxia. J Control Release 2011;156:276.
15. Schweitzer C, Schmidt R. Physical mechanisms of generation and deactivation of singlet oxygen. Chem Rev 2003;103:1685.
16. Sternberg ED, Dolphin D, Brickner C. Porphyrin-based photosensitizers for use in photodynamic therapy. Tetrahedron 1998;54:4151.
17. Tada D, Vono L, Duarte E, et al. Methylene blue-containing silica-coated magnetic particles: A potential

magnetic carrier for photodynamic therapy. Langmuir 2007;23:8194.
18. Qin M, Hah HJ, Kim G, et al. Methylene blue covalently loaded polyacrylamide nanoparticles for enhanced tumor-targeted photodynamic therapy. Photochem Photobiol Sci 2011;10:832.
19. McLear PW, Hayden RE. Prevention of cutaneous phototoxicity in photodynamic therapy. Am J Otolaryngol 1989; 10:92.
20. Weishaupt KR, Gomer CJ, Dougherty TJ. Identification of singlet oxygen as the cytotoxic agent in photo-inactivation of a murine tumor. Cancer Res 1976;36, 2326.
21. Chen T-C, Huang L, Liu C-C, et al. Luminol as the light source for *in situ* photodynamic therapy. Process Biochem 2012;47:1903.
22. Turgut B, Vural O, Pala FS, et al. 17p Deletion is associated with resistance of B-cell chronic lymphocytic leukemia cells to *in vitro* fludarabine-induced apoptosis. Leuk Lymphoma 2007;48, 311.
23. Parikh SA, Rabe KG, Kay NE, et al. Chronic lymphocytic leukemia in young (< = 55 years) patients: A comprehensive analysis of prognostic factors and outcomes. Haematologica 2014;99:140.
24. Boudreau RTM, Conrad DM, Hoskin DW. Differential involvement of reactive oxygen species in apoptosis caused by the inhibition of protein phosphatase 2A in Jurkat and CCRF-CEM human T-leukemia cells. Exp Mol Pathol 2007;83:347.
25. Pelicano H, Feng L, Zhou Y, et al. Inhibition of mitochondrial respiration: A novel strategy to enhance drug-induced apoptosis in human leukemia cells by a reactive oxygen species-mediated mechanism. J Biol Chem 2003;278:37832.
26. Gollmer A, Arnbjerg J, Blaikie FH, et al. Singlet Oxygen Sensor Green®: Photochemical behavior in solution and in a mammalian cell. Photochem Photobiol 2011;87:671.
27. Scurlock RD, Wang B, Ogilby PR. Chemical reactivity of singlet sigma oxygen (b 1 Σ g+) in solution. J Am Chem Soc 1996;118:388.
28. Weldon D, Ogilby PR. Time-resolved absorption spectrum of singlet oxygen in solution. J Am Chem Soc 1998;120: 12978.
29. Marina A. Orlova, Osipova EY, Roumiantsev SA. Effect of 67Zn-nanoparticles on leukemic cells and normal lymphocytes. British J Med Med Res 2012;2:21
30. Young RH, Wehrly K, Martin RL. Solvent effects in dye-sensitized photooxidation reactions. J Am Chem Soc 1971;93: 5774.
31. Abdulmalik A, Hibah A, Zainy BM, et al. Preparation of soluble stable C_{60}/human serum albumin nanoparticles via cyclodextrin complexation and their reactive oxygen production characteristics. Life Sci 2013;93:277.
32. Bihari P, Vippola M, Schultes S, et al. Optimized dispersion of nanoparticles for biological *in vitro* and *in vivo* studies. Part Fibre Toxicol 2008;5:14.
33. Tan TL, Lai CW, Abd Hamid SB. Tunable band gap energy of Mn-doped ZnO nanoparticles using the coprecipitation technique. J Nanomater 2014;2014:1.
34. Jana S, Srivastava BB, Jana S, et al. Multifunctional doped semiconductor nanocrystals. J Phys Chem Lett 2012;3: 2535.
35. Porambo MW, Howard HR, Marsh AL. Dopant effects on the photocatalytic activity of colloidal zinc sulfide semiconductor nanocrystals for the oxidation of 2-chlorophenol. J Phys Chem C 2010;114:1580.
36. Srivastava BB, Jana S, Karan NS, et al. Highly luminescent Mn-doped ZnS nanocrystals: Gram-scale synthesis. J Phys Chem Lett 2010;1:1454.
37. Geszke M, Murias M, Balan L, et al. Folic acid-conjugated core/shell ZnS:Mn/ZnS quantum dots as targeted probes for two photon fluorescence imaging of cancer cells. Acta Biomater 2011;7:1327.
38. Jiang D, Cao L, Liu W, et al. Synthesis and luminescence properties of core/shell ZnS:Mn/ZnO nanoparticles. Nanoscale Res Lett 2009;4:78.
39. Abts H, Emmerich M, Miltenyi S, et al. CD20 positive human B lymphocytes separated with the magnetic cell sorter (MACS) can be induced to proliferation and antibody secretion *in vitro*. J Immunol Methods 1989;125:19.
40. DeRosa MRC. Photosensitized singlet oxygen and its applications. Coord Chem Rev 2002;233–234:351.
41. Miller JS. Rose Bengal-sensitized photooxidation of 2-chlorophenol in water using solar simulated light. Water Res 2005;39:412.
42. Kostka M, Zimcik P, Miletin M, et al. Comparison of aggregation properties and photodynamic activity of phthalocyanines and azaphthalocyanines. J Photochem Photobiol A Chem 2006;178:16.
43. Mansilla E, Marin G, Núñez L. Present and future application of nanoparticle based therapies in B-chronic lymphocytic leukemia (B-CLL). In *intechopen.com*, 2012, pp. 431–448. Available at: www.intechopen.com/source/pdfs/28000/InTech-Present_and_future_application_of_nanoparticle_based_therapies_in_b_chronic_lymphocytic_leukemia_b_cll_.pdf Accessed: June 30, 2014.
44. Akhtar MJ, Ahamed M, Kumar S, et al. Zinc oxide nanoparticles selectively induce apoptosis in human cancer cells through reactive oxygen species. Int J Nanomedicine 2012; 7:845.
45. Baptista MS, Indig GL. Effect of BSA binding on photophysical and photochemical properties of triarylmethane dyes. J Phys Chem B 1998;102:4678.
46. Kraljić I, Mohsni S. El. A new method for the detection of singlet oxygen in aqueous solutions. Photochem Photobiol 1978;28:577.
47. Wilkinson F, Helman W, Ross A. Quantum yields for the photosensitized formation of the lowest electronically excited singlet state of molecular oxygen in solution. J Phys Chem 1993;113:1.
48. Onoue S, Yamauchi Y, Kojima T, et al. Analytical studies on photochemical behavior of phototoxic substances; effect of detergent additives on singlet oxygen generation. Pharm Res 2008;25:861.
49. Triesscheijn M, Baas P, Schellens JHM, et al. Photodynamic therapy in oncology. Oncologist 2006;11:1034.
50. Wang HJ, Shrestha R, Zhang Y. Encapsulation of photosensitizers and upconversion nanocrystals in lipid micelles for photodynamic therapy. Part Part Syst Charact 2014;31:228.
51. Chatterjee DK, Fong LS, Zhang Y. Nanoparticles in photodynamic therapy: An emerging paradigm. Adv Drug Deliv Rev 2008;60:1627.
52. Samia ACS, Chen X, Burda C. Semiconductor quantum dots for photodynamic therapy. J Am Chem Soc 2003;125:15736.
53. Bakalova R, Ohba H, Zhelev Z, et al. Quantum dots as photosensitizers? Nat Biotechnol 2004;22:1360.
54. Zhang P, Steelant W, Kumar M, et al. Versatile photosensitizers for photodynamic therapy at infrared excitation. J Am Chem Soc 2007;129:4526.